ingegneria sismica
International Journal of Earthquake Engineering
Anno XLIII - Num. 1 - 2026

Research on Market Mechanism and Regulation Strategy of Aggregate Class Electricity Subjects in High Proportion Renewable Energy Power System

Miao Wang[1], *Zijiao Han*[1], *Sichen Lu*[1], *Yanyun Zhang*[2,*], *Yubo Jia*[2] *and Mingshun Ji*[2]

[1] State Grid Liaoning Electric Power Co., ltd., Shenyang, Liaoning, 110006, China
[2] Beijing Tsintergy Technology Co., Ltd., Beijing, 100080, China

SUMMARY: *The stochastic, intermittent and fluctuating characteristics of wind and photovoltaic power generation make the stable operation of a high percentage of renewable energy power systems potentially risky. The market mechanism and regulation strategy of the power system are important means to ensure the stable and reliable operation of the system. In this paper, wind turbines, gas turbines, energy storage and load and a high proportion of renewable energy are aggregated into a power plant, and the power plant is considered to participate in the multi-species trading consisting of the energy market, demand response market and frequency regulation market, and the optimal regulation model and regulation strategy of the power plant is established by considering the impact of the appraisal mechanism and the multiple uncertainty factors. Then a multi-objective particle swarm algorithm based on the dynamic collaboration of multiple swarms is proposed, and the optimal regulation strategy is obtained by solving the model using the DCMOPSO algorithm. The experiment is based on the node system to verify the model proposed in this paper, and it is found that the wind energy storage plant participates in the market with lower offer price, while in the DAM scenario, it participates in the market before the day of the market with higher market offer price, and at the same time, with the enhancement of its own offer price, the market price of electricity will be increased accordingly. It is verified that the method proposed in this paper can optimize the offer strategy of power storage stations and enrich the energy storage regulation means.*

KEYWORDS: *market mechanism; regulation model; DCMOPSO; power system; high proportion of renewable energy sources*

1 Introduction

Under the dual-carbon background, the clean and low-carbon transformation speed of China's power system is showing a steady upward trend, and a high proportion of renewable energy power system is gradually coming into the public's view [1, 2]. On the one hand, the rapid development and wide application of renewable energy sources such as wind power and photovoltaic have made the design and development of China's power structure move in the direction of decarbonization [3, 4]; on the other hand, with the gradual expansion of the scale of distributed resources such as energy storage, electric vehicles, controllable loads and other highly flexible nature, the support level of China's power grid has been effectively enhanced [5, 6]. However, the high proportion of renewable energy sources is inherently unstable and intermittent, which poses a serious challenge to the stability and reliability of the power grid

*zhangyany@tsintergy.com
https://doi.org/10.65102/is2026240
Published: 30 April, 2026

[7]. As an important strategy to effectively deal with these problems [8, 9], virtual power plants and other aggregated power subjects have become an important topic in current power system research by stimulating the potential of aggregated power subjects and formulating effective regulation strategies through market mechanisms.

On the one hand, the daily and hourly scheduling hierarchy is the basic framework. In the case of a high proportion of renewable energy, the daily Ahead program needs to fully consider the uncertainty of wind and light forecasts and leave the necessary flexibility reserves [10, 11]; real-time dispatch undertakes a quick response to sudden changes, tries to adjust the output through market and technical means, and avoids the cost increase and system pressure brought by large-scale redispatch [12, 13]. To this end, it is necessary to establish a set of integrated dispatch mechanisms covering unit decision-making, energy storage utilization, load response and cross-area coordination. The second is the effective management of forecasts and uncertainties [14]. Renewable energy output is often weather-driven and forecast errors are inevitable [15]. In order to reduce the risk, scheduling needs to transform the forecast results into a more informative decision basis by giving not only a definite output value, but also uncertainty intervals, probability distributions, or multi-scenario combinations [16]. Through scenario analysis, the cost and risk of different weather scenarios can be assessed clearly at the day Ahead stage, and the response strategy can be determined in advance [17, 18]. In actual operation, wind and light forecasts and demand forecasts should be deeply coupled, and a cross-regional data sharing mechanism should be established to allow regions to make collaborative decisions under the same information context [19-21].

The article firstly constructs an optimized regulation model for power plants to participate in power spot market transactions according to the relevant rules of power spot market transactions. Then, it proposes an optimal regulation strategy for power plants to participate in multi-species trading under the environment of power spot market. Scenario planning method and conditional value-at-risk are utilized to deal with the impacts caused by the uncertainty of wind turbines, loads, tariffs and FM signals. On this basis, the DCMOPSO algorithm is introduced to find the optimal solution set of the power generation system to solve the optimal regulation strategy. Subsequently, the performance of the improved multi-objective particle swarm optimization algorithm and other intelligent algorithms are tested and compared on the set of benchmark functions. Finally, a nodal system is used as an example to verify the effectiveness of the market optimization and regulation method proposed in this paper.

2 Method

2.1 Optimized regulation model for power plant aggregation class of power subjects

2.1.1 Optimizing the regulatory process

The trading varieties that power plants can participate in under the power spot market environment include demand response, FM auxiliary services, and spot power energy market transactions. The optimized regulation process of power plant participating in multi-variety transactions is shown in Figure 1. First of all, the power plant in the day before the stage to receive demand response day before the invitation, combined with all kinds of internal resources and market information forecasts for the next day, to the market declaration of the next day 24 hours of the energy curve, the previous demand response and FM capacity. In this paper, it is assumed that the power plant participates in the power market transactions at the market clearing price to settle the relevant costs and benefits. Secondly, in the real-time phase,

the power plant determines the specific upward or downward FM strategy for each phase of the 5 min time scale within 1 h according to the real-time demand response invitation information, its own capacity margin and real-time price fluctuations.

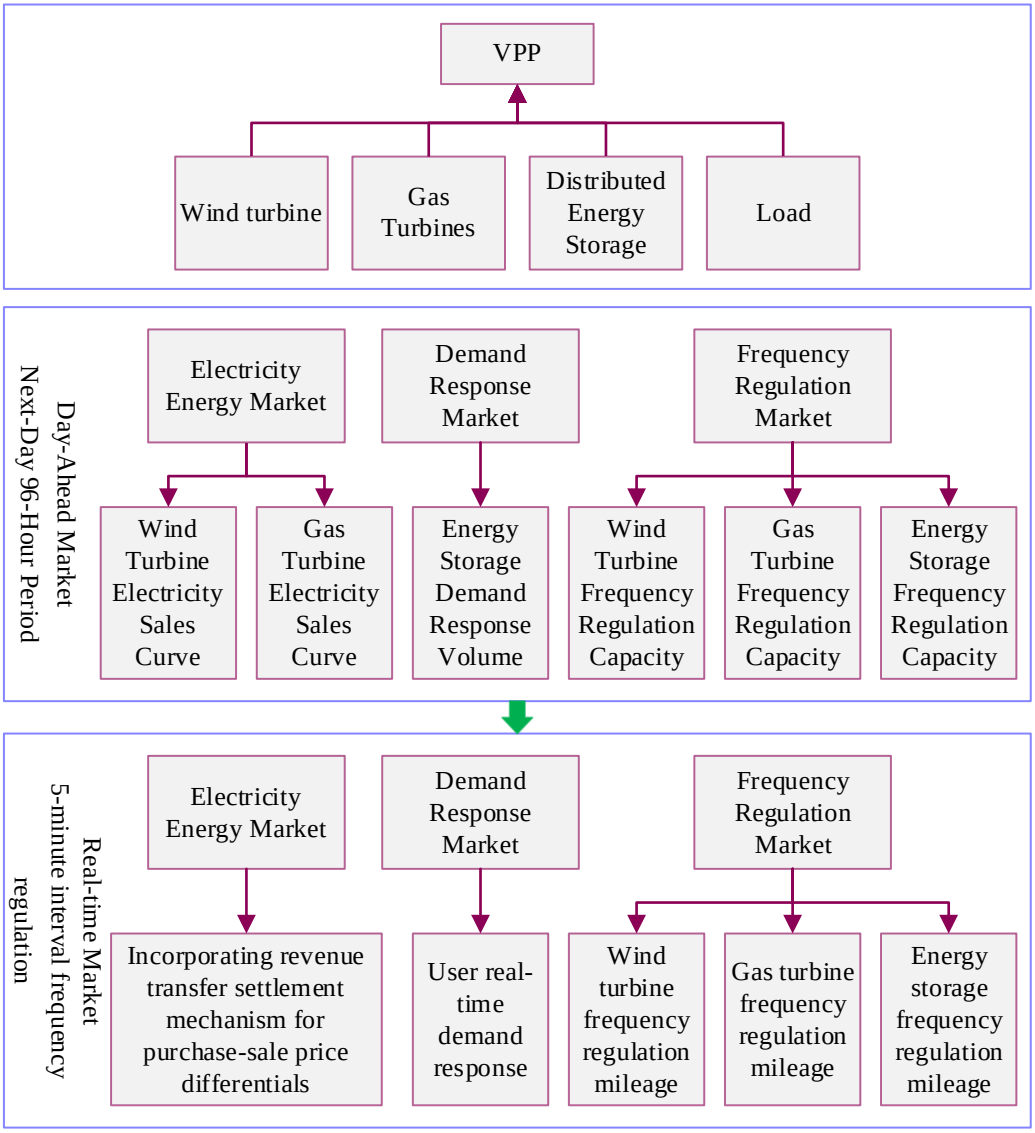

Figure 1: The optimized regulation process for power plants' participation

2.1.2 Optimizing regulatory models

According to the relationship between various types of resource power within the power plant and market demand, the corresponding multi-timescale optimization and regulation model is established, as shown in equation (1).

$$\begin{cases} P_{load,t} = P_{mt,t}^{own} + P_{wd,t}^{own} + P_{ess,t}^{dis} - P_{ess,t}^{cha} \\ P_{fr,t}^{cap} \le P_{mt,t}^{fr,cap} + P_{wd,t}^{fr,cap} + P_{ess,t}^{fr,cap} \end{cases} \quad (1)$$

where: $P_{load,t}$ is the predicted value of the internal load of the plant at each stage of t moment. $P_{mt,t}^{own}$, $P_{wd,t}^{own}$ are the values of gas turbine and wind turbine used for the internal supply load

of the power plant for each stage of t moment of dissipation, respectively. $P_{ess,t}^{cha}$, $P_{ess,t}^{dis}$ are the charging and discharging power of the energy storage at each stage t moment, respectively. $P_{fr,t}^{cap}$ is the value of FM capacity required by the FM market at each stage t moment. $P_{mt,t}^{fr,cap}$, $P_{wd,t}^{fr,cap}$ and $P_{ess,t}^{fr,cap}$ are the values of the FM capacity allocated to gas turbines, wind turbines and energy storage at the moment of each stage t, respectively.

2.2 Optimize the regulation strategy

2.2.1 Earlier stages

(1) Objective function

$$\max F_{da} = \sum_{n=1}^{N}\sum_{t=1}^{T} \omega_n \left(Q_{pm,t}^{da,n} + Q_{fr,t}^{da,n} + Q_{dr,t}^{da,n} - C_{mt,t}^{da,n} - C_{ess,t}^{da,n} - C_{res,t}^{da,n} \right) - C_{CVaR}^{da} \tag{2}$$

where: N and T are the number of scenes and the number of time periods, respectively. ω_n is the scene probability. $Q_{dr,t}^{da,n}$, $Q_{fr,t}^{da,n}$, and $Q_{pm,t}^{da,n}$ are the demand response revenues, FM revenues, and power sales revenues of the power plant, respectively. $C_{mt,t}^{da,n}$, $C_{\mathrm{ess},t}^{da,n}$ are the outage costs of gas turbines and energy storage, respectively. $C_{\mathrm{res},t}^{da,n}$ is the conventional standby cost of the plant. C_{CVaR}^{da} is the CVaR revenue risk cost of the power plant, which is calculated as shown in equation (3).

$$\begin{cases} Q_{pm,t}^{da,n} = \lambda_{pm,t}^{da,n} \left(P_{da,mt,t}^{n,pm} + P_{da,wd,t}^{n,pm} \right) \\ Q_{fr,t}^{da,n} = \lambda_{fr,t}^{da,n} \left(P_{da,t}^{n,fr,up} + P_{da,t}^{n,fr,dn} \right) \\ Q_{dr,t}^{da,n} = \lambda_{dr,t}^{da,n} \left(P_{ess,t}^{n,cha} - P_{ess,t}^{n,dis} - P_{base,t}^{n,da} \right) \\ C_{mt,t}^{da,n} = P_{mt,t}^{n} \sum_{i=1}^{I} \alpha_i \left(B_i + Q_i \right) \\ C_{ess,t}^{da,n} = C_{ess} \left(P_{ess,t}^{n,dis} + P_{ess,t}^{n,cha} \right) \\ C_{res,t}^{da,n} = C_{res,mt} \left(P_{mt,t}^{n,res,+} + P_{mt,t}^{n,res,-} \right) + C_{res,ess} \left(P_{ess,t}^{n,res,+} + P_{ess,t}^{n,res,-} \right) \\ C_{CVaR}^{da} = \mu^{da} \left[\zeta_{da} - \dfrac{1}{N\left(1-\beta_{da}\right)} \right] \sum_{n=1}^{N} z_n^{da} \end{cases} \tag{3}$$

where: $\lambda_{pm,t}^{da,n}$, $\lambda_{fr,t}^{da,n}$ and $\lambda_{dr,t}^{da,n}$ are the market price of purchased and sold power, FM capacity and demand response, respectively. C_{ess} is the charging and discharging cost of energy storage. $C_{res,mt}$, $C_{res,ess}$ are the standby opportunity costs of gas turbines and energy storage, respectively. α_i, B_i and Q_i are the emission intensity, penalty order of magnitude and environmental value of the gas unit gas, respectively. $P_{mt,t}^{n}$ is the power of the gas turbine. $P_{ess,t}^{n,cha}$ and $P_{ess,t}^{n,dis}$ are the charging and discharging power of the energy storage, respectively. $P_{da,mt,t}^{n,pm}$ and $P_{da,wd,t}^{n,pm}$ are the power sold by gas turbines and wind turbines, respectively. $P_{da,t}^{n,fr,up}$

and $P_{da,t}^{n,fr,dn}$ are the upward and downward FM capacity of the plant, respectively, which is calculated as shown in equation (4). $P_{mt,t}^{n,\mathrm{res},+}$, $P_{mt,t}^{n,\mathrm{res},-}$, $P_{\mathrm{ess},t}^{n,\mathrm{res},+}$, $P_{\mathrm{ess},t}^{n,\mathrm{res},-}$ for the Positive and negative conventional standby capacity of gas turbine, energy storage. $P_{\mathrm{base},t}^{n,da}$ is the baseline load for the day-ahead phase. μ^{da} is the risk appetite factor. β_{da} is the confidence level. ζ_{da} and z_n^{da} are auxiliary variables.

$$\begin{cases} P_{da,t}^{n,fr,up} = P_{da,mt,t}^{n,fr,up} + P_{da,\mathrm{ess},t}^{n,fr,up} \\ P_{da,t}^{n,fr,dn} = P_{da,mt,t}^{n,fr,dn} + P_{da,\mathrm{ess},t}^{n,fr,dn} + P_{da,wd,t}^{n,fr,dn} \end{cases} \tag{4}$$

where: $P_{da,mt,t}^{n,fr,up}$, $P_{da,\mathrm{ess},t}^{n,fr,up}$ are the upward FM capacities of the gas turbine and the storage determined in the day-ahead stage, respectively. $P_{da,mt,t}^{n,fr,dn}$, $P_{da,\mathrm{ess},t}^{n,fr,dn}$, and $P_{da,wd,t}^{n,fr,dn}$ are the downward FM capacities determined at the day-ahead stage for the gas turbine, the energy storage, and the WT respectively.

(2) Constraints

(1) Gas turbine constraints

Eq. (5) is the gas turbine equation constraint, Eq. (6) is the gas turbine unit output upper and lower limit constraints, Eq. (7) represents the gas turbine unit FM capacity constraints, Eq. (8) is the gas turbine unit creep constraints, and Eq. (9) is the gas turbine unit conventional standby capacity constraints.

$$P_{mt,t}^{n} = P_{da,mt,t}^{n,pm} + P_{mt,t}^{n,own} + P_{mt,t}^{n,res,-} + P_{da,mt,t}^{n,fr,dn} \tag{5}$$

$$0 \le P_{mt,t}^{n} \le u_{mt,t}\left(P_{mt,t}^{\max} - P_{da,mt,t}^{n,fr,up} - P_{mt,t}^{n,res,+}\right) \tag{6}$$

$$\begin{cases} 0 \le P_{da,mt,t}^{n,fr,up} \le \min\left(u_{mt,t}k_{mt}, P_{mt,t}^{\max} - P_{mt,t}^{n,res,+} - P_{mt,t}^{n}\right) \\ 0 \le P_{da,mt,t}^{n,fr,dn} \le \min\left(u_{mt,t}k_{mt}, P_{mt,t}^{n} - P_{mt,t}^{n,res,-}\right) \end{cases} \tag{7}$$

$$-k_{mt} \le P_{mt,t+1}^{n} - P_{mt,t}^{n} \le k_{mt} \tag{8}$$

$$\begin{cases} \alpha_{mt,t}^{\mathrm{res,min}} P_{mt,t}^{\max} \le P_{mt,t}^{n,\mathrm{res},+} \le \Delta_{mt}k_{mt} \\ \alpha_{mt,t}^{\mathrm{res,min}} P_{mt,t}^{\max} u_{mt,t}^{n} \le P_{mt,t}^{n,\mathrm{res},-} \le \Delta_{mt}k_{mt}u_{mt,t}^{n} \end{cases} \tag{9}$$

where: $u_{mt,t}^{n}$ is the 0-1 start-stop state variable of the gas turbine unit. $P_{mt,t}^{\max}$ is the upper limit of gas turbine unit output. k_{mt} is the maximum climb value of the gas turbine unit. $\alpha_{mt,t}^{\mathrm{res,min}}$ is the minimum scaling requirement for conventional standby capacity. Δ_{mt} is the length of time for the gas unit to activate the standby capacity in advance, often taken as 4h.

(2) Energy storage constraints

Eq. (10) and Eq. (11) are energy storage charging and discharging power constraints, Eq. (12) is energy storage SOC value change constraints, and Eq. (13) and Eq. (14) are energy storage FM capacity and conventional standby capacity constraints.

$$\begin{cases} 0 \le P_{\mathrm{ess},t}^{n,\mathrm{dis}} \le u_{\mathrm{ess},t}^{n,\mathrm{dis}} P_{\mathrm{ess},t}^{\mathrm{dis,max}} \\ 0 \le P_{\mathrm{ess},t}^{n,\mathrm{cha}} \le u_{\mathrm{ess},t}^{n,\mathrm{cha}} P_{\mathrm{ess},t}^{\mathrm{cha,max}} \end{cases} \tag{10}$$

$$u_{\mathrm{ess},t}^{n,\mathrm{dis}} + u_{\mathrm{ess},t}^{n,\mathrm{cha}} = 1 \tag{11}$$

$$SOC_{ess,t+1}^{n} = \left[\left(\eta_{ess}^{cha} P_{ess,t}^{n,cha} - P_{ess,t}^{n,dis} / \eta_{ess}^{dis} \right) \Delta t_{da} \right] \Big/ C_{ess}^{Cap} + SOC_{ess,t}^{n} \left(1 - \delta_{ess} \right) \tag{12}$$

$$\begin{cases} 0 \le P_{da,ess,t}^{n,fr,up} + P_{ess,t}^{n,res,+} \le P_{ess,t}^{dis,\max} - P_{ess,t}^{n} \\ 0 \le P_{da,ess,t}^{n,fr,dn} + P_{ess,t}^{n,res,-} \le P_{ess,t}^{cha,\max} + P_{ess,t}^{n} \end{cases} \tag{13}$$

$$\begin{cases} P_{ess,t}^{n,res,+} \Delta t \ge \alpha_{es,res}^{\min,+} S \left(SOC_{ess}^{\max} - SOC_{ess}^{\min} \right) \\ P_{ess,t}^{n,res,-} \Delta t \ge \alpha_{es,res}^{\min,-} S \left(SOC_{ess}^{\max} - SOC_{ess}^{\min} \right) \end{cases} \tag{14}$$

where: $u_{ess,t}^{n,cha}$, $u_{ess,t}^{n,dis}$ are the charging and discharging state variables of the energy storage, respectively. $P_{ess,t}^{cha,\max}$, $P_{ess,t}^{dis,\max}$ are the charging and discharging power of the energy storage, respectively. $\mathrm{SOC}_{\mathrm{ess},t}^{n}$ is the SOC value of the energy storage. $\mathrm{SOC}_{\mathrm{ess},m}^{\max}$, $\mathrm{SOC}_{\mathrm{ess}}^{\min}$ are the SOC maximum and minimum limits of the energy storage, respectively. $\eta_{\mathrm{ess}}^{\mathrm{cha}}$, $\eta_{\mathrm{ess}}^{\mathrm{dis}}$ are the charging and discharging efficiencies of the energy storage, respectively. δ_{ess}, $C_{\mathrm{ess}}^{\mathrm{Cap}}$ are the self-discharge rate and capacity of the energy storage, respectively. $\alpha_{es,\mathrm{res}}^{\min,+}$, $\alpha_{es,\mathrm{res}}^{\min,-}$ are the minimum ratio values of positive and negative conventional standby capacity of the energy storage, respectively. S is the total installed capacity of energy storage. Δt_{da} is the day-ahead phase regulation time scale, taken as 1h.

(3) Wind turbine constraints

Equation (15) is the WTG power constraint.

$$P_{wd,t}^{n} = P_{wd,t}^{n,\mathrm{own}} + P_{da,wd,t}^{n,pm} + P_{da,wd,t}^{n,fr,dn} \tag{15}$$

4) Power plant constraints

The overall capacity declaration constraints and internal energy balance constraints of the power plant are shown in Eq. (1).The CVaR constraints are shown in Eq. (16).

$$\begin{cases} z_n^{da} \ge 0 \\ z_n^{da} \ge \zeta_{da} - \left(Q_{pm,t}^{da,n} + Q_{dr,t}^{da,n} \right) \end{cases} \tag{16}$$

2.2.2 Real-time phase

(1) Objective function

The objective function equation is shown in (17).

$$\max F_{rt} = \sum_{n=1}^{N} \sum_{t=1}^{T} \omega_n \left(Q_{dr,t}^{rt,n} + Q_{fr,t}^{rt,n} - \Delta C_{pm,t}^{rt,n} \right) - C_{CVaR}^{rt} \tag{17}$$

where: $Q_{dr,t}^{rt,n}$, $Q_{fr,t}^{rt,n}$ are the demand response gain and FM mileage gain in the real-time phase, respectively. $\Delta C_{pm,t}^{rt,n}$, C_{CVaR}^{rt} are the power purchase and sale deviation penalty cost and CVaR cost in real-time phase, respectively, and the specific calculations of the rest of the benefits or costs are shown in Eq. (18), Eq. (19) and Eq. (3), respectively.

$$\begin{cases} Q_{fr,t}^{rt,n} = \lambda_{fr,t}^{rt,n} k_{rt} \left(P_{da,t}^{n,fr,up} \alpha_{da,t}^{fr,up} + P_{da,t}^{n,fr,dn} \alpha_{da,t}^{fr,dn} \right) \\ k_{rt} = 0.25\left(2k_1 + k_2 + k_3^+ + k_3^- \right) \\ k_3^+ = 1 - \left| \Delta P_{rt,t}^{n,fr,up} - P_{da,t}^{n,fr,up} \alpha_{da,t}^{fr,up} \right| \Big/ \left(\alpha_{cap}^{\max} P_{cap} \right) \\ k_3^- = 1 - \left| \Delta P_{rt,t}^{n,fr,dn} - P_{da,t}^{n,fr,dn} \alpha_{da,t}^{fr,dn} \right| \Big/ \left(\alpha_{cap}^{\max} P_{cap} \right) \end{cases} \tag{18}$$

where: $\lambda_{fr,t}^{rt,n}$ is the FM mileage price in the real-time phase. $\alpha_{da,t}^{fr,up}$, $\alpha_{da,t}^{fr,dn}$ are the scalar values of upward and downward FM demand in the real-time phase, respectively. k_1, k_2, k_3^+ and k_3^- are the FM rate, response time, upward and downward FM accuracy respectively. $\Delta P_{rt,t}^{n,fr,up}$, $\Delta P_{rt,t}^{n,fr,dn}$ are the upward and downward FM mileage in real-time phase, respectively. $\alpha_{\text{cap}}^{\max}$, P_{cap} are the maximum permissible error in FM and the total authorized capacity of FM resources of the power plant, respectively.

$$\Delta C_{pm,t}^{rt,n} = \begin{cases} \left(\lambda_{pm,t}^{rt,n} - \lambda_{pm,t}^{da,n} \right) \left[P_{da,t}^{n,pm} - P_{rt,t}^{n,pm} \left(1 + \alpha_{err} \right) \right] \\ P_{da,t}^{n,pm} > P_{rt,t}^{n,pm} \left(1 + \alpha_{err} \right) \cap \lambda_{pm,t}^{rt,n} > \lambda_{pm,t}^{da,n} \\ \left(\lambda_{pm,t}^{da,n} - \lambda_{pm,t}^{rt,n} \right) \left[P_{rt,t}^{n,pm} \left(1 - \alpha_{err} \right) - P_{da,t}^{n,pm} \right] \\ P_{da,t}^{n,pm} < P_{rt,t}^{n,pm} \left(1 - \alpha_{err} \right) \cap \lambda_{pm,t}^{rt,n} < \lambda_{pm,t}^{da,n} \end{cases} \tag{19}$$

where: $\lambda_{pm,t}^{rt,n}$ is the price of electricity purchased and sold in the real-time phase. $P_{rt,t}^{n,pm}$ is the declared electricity sales in the real-time phase. α_{err} is the maximum allowable deviation rate. $P_{rt,t}^{n,pm}$ is calculated as shown in equation (20).

$$\begin{cases} \Delta P_{rt,t}^{n,fr,up} = \Delta P_{rt,mt,t}^{n,fr,up} + \Delta P_{rt,ess,t}^{n,fr,up} \\ \Delta P_{rt,t}^{n,fr,dn} = \Delta P_{rt,mt,t}^{n,fr,dn} + \Delta P_{rt,ess,t}^{n,fr,dn} + \Delta P_{rt,wd,t}^{n,fr,dn} \\ P_{rt,t}^{n,pm} = P_{rt,mt,t}^{n,pm} + P_{rt,wd,t}^{n,pm} \end{cases} \tag{20}$$

where: $\Delta P_{rt,mt,t}^{n,fr,up}$, $\Delta P_{rt,\text{ess},t}^{n,fr,up}$ are the upward FM mileage of the gas turbine and the energy storage in the real-time phase, respectively. $\Delta P_{rt,mt,t}^{n,fr,dn}$, $\Delta P_{rt,\text{ess},t}^{n,fr,dn}$ and $\Delta P_{rt,wd,t}^{n,fr,dn}$ are the downward FM mileage in real-time stage for gas turbines, energy storage and wind turbines respectively. $P_{rt,mt,t}^{n,pm}$ and $P_{rt,wd,t}^{n,pm}$ are the electricity sales of gas turbines and wind turbines in the real-time phase, respectively.

(2) Constraints

1) Gas turbine constraints

Equation (21) is the gas turbine FM mileage constraint.

$$\begin{cases} \Delta P_{rt,mt,t}^{n,fr,up} \le \min\left(k_{mt}\Delta t_{fr,rt}, P_{da,mt,t}^{n,fr,up}\right) \\ \Delta P_{rt,mt,t}^{n,fr,dn} \le \min\left(k_{mt}\Delta t_{fr,rt}, P_{da,mt,t}^{n,fr,dn}\right) \end{cases} \tag{21}$$

where: $\Delta t_{fr,rt}$ is the 5min FM time scale of the real-time phase.

2) Energy storage constraints

Eq. (22) is the energy storage FM mileage constraint, and Eq. (23) is the SOC constraint of energy storage in real-time phase.

$$\begin{cases} 0 \le \Delta P_{rt,ess,t}^{n,fr,up} \le u_{rt,ess,t}^{n,fr,up} P_{ess,m,t}^{n,fr,up} \\ 0 \le \Delta P_{rt,ess,t}^{n,fr,dn} \le u_{rt,ess,t}^{n,fr,dn} P_{ess,m,t}^{n,fr,dn} \end{cases} \tag{22}$$

$$\begin{aligned} SOC_{ess,m,t+1}^{n} = &\left[\left(\eta_{ess}^{cha}\Delta P_{rt,ess,t}^{n,fr,dn} - \Delta P_{rt,ess,t}^{n,fr,up}/\eta_{ess}^{dis}\right)\Delta t\right]\Big/ C_{ess}^{Cap} \\ &+ SOC_{ess,m,t}^{n}\left(1-\delta_{ess}\right) \end{aligned} \tag{23}$$

where: $u_{rt,\mathrm{ess},t}^{n,fr,up}$, $u_{rt,\mathrm{ess},t}^{n,fr,dn}$ are the upward and downward FM state variables of the energy storage, respectively.

(3) Wind turbine constraints

Eq. (24) is the downward FM mileage constraint of the WTG.

$$\Delta P_{rt,wd,t}^{n,fr,dn} \le P_{da,wd,t}^{n,fr,dn} \tag{24}$$

4) Power plant constraints

The overall capacity declaration constraints and internal energy balance constraints of the power plant are shown in Equation (1) and the CVaR constraints are shown in Equation (16).

2.3 Multi-objective particle swarm algorithm based on dynamic synergy of multiple swarms

2.3.1 Particle Swarm Optimization

The algorithm to find the best among them on the basis of random search in the population is the particle swarm optimization algorithm. In order to find the best position in the space, the search is done in the space in the form of bird movement. Individuals of the population make up its searching individuals, i.e. particles, including both position and velocity information. When there is N particle in the present population, the search is performed in n-dimensional hyperspace. For particle $i \in (1,2,\cdots,N)$, its position is $x_i = (x_{i1}, x_{i2}, \cdots, x_{in})$ and velocity is $v_i = (v_{i1}, v_{i2}, \cdots, v_{in})$. The particle is updated with Eq:

$$v_i(t+1) = w \times v_i(t) + c_1 r_1\left(x_{pbest_i} - x_i(t)\right) + c_2 r_2\left(x_{gbest_i} - x_i(t)\right) \tag{25}$$

$$x_i(t+1) = x_i(t) + v_i(t+1) \tag{26}$$

where: t represents the number of iteration generations. w represents the inertia factor, which determines whether its search scope is local or global; a high value of w searches

globally and a low value searches locally. The convergence rates are c_1 and c_2, respectively. The random quantities are r_1, r_2 in $(0,1)$ normal distribution. The individual and global optimal solutions are pbest and gbest, respectively. there are many global optimal solutions for the multi-objective particle swarm algorithm, so we can find the most optimal one in other domains, nbest, and use nbest as a substitute. Rewrite equation (25) as:

$$v_i(t+1) = w \times v_i(t) + c_1 r_1 \left(x_{pbest_i} - x_i(t) \right) + c_2 r_2 \left(x_{nbest_i} - x_i(t) \right) \tag{27}$$

2.3.2 Strategies for Improving the Multi-Objective Particle Swarm Algorithm

(1) Multi-population strategy

In order to improve the algorithm in terms of searchability and convergence, more than one population can be utilized by incorporating multiple swarm strategies to solve the problem and achieve good results. Initialize U populations DCMOPSO where the number of particles is N. For the population its evolution process is independent and the position $x_k^t(i,j)\left(k=1,2,\cdots,N\right)$ and velocity $v_k^t(i,j)$ of each particle in the evolution are recorded.

(2) Dynamic clustering strategy

As evolution proceeds, the population will gradually lose its diversity, resulting in local optimization, in order to maintain the diversity of the population, a dynamic clustering strategy is needed. Under the condition of t th generation, the dynamic clustering strategy is carried out in the following way:

1) Dynamic clustering is applied to the k th population, and in particle ordering, the order is determined according to the relationship of sparse distance, rather than dictating its ordering.

2) The populations are categorized according to high-quality and poor-quality clusters. The high-quality population accepts only particles with a threshold δ, while other particles are inferior. The particles are to be distributed to in each subpopulation, and the following form of δ is calculated and varied:

$$\delta = t / T \tag{28}$$

$$\delta = 1/\left(1+e^{ratio}\right) \tag{29}$$

$$ratio = e^{0.9\times f_r} - 1 \tag{30}$$

where: the number of iterations is t, the threshold change ratio is ratio. the number of empty subpopulations appearing is f_r.

3) When the particles finish updating, the sub-populations are unified into one population, and a new population is found in it to continue to undertake the dynamic clustering strategy in the future.

(3) Speed update of particles

Then the k th population is dynamically divided, where the number of particles in the high-quality population is E and the number of particles in the low-quality population is $N-E$. The update of particles is as follows:

The velocity equation of the quality swarm is:

$$\begin{aligned} v_H^{t+1}(i,j) &= wv_H^t(i,j) + c_1 r_1 \left(P_{best_H}^t(i,j) - x_H^t(i,j) \right) \\ &+ c_2 r_2 \left(Y_{best_H}^t(i,j) - x_H^t(i,j) \right) \\ &k = 1,2,\cdots,U; \\ &i = 1,2,\cdots,E; \\ &j = 1,2,\cdots,D \end{aligned} \tag{31}$$

where: $x_H^t(i,j)$ represents the j th dimension of the current position of particle i for the current quality swarm. $P_{bestH}^t(i,j)$ is the j th dimension of particle i's P_{best}. $Y_{bestH}^t(i,j)$ represents the j th dimension of the optimal particle. When the particle is the only one, the position of that particle is Y_{bestH}.

The velocity equation of the inferior swarm is:

$$\begin{aligned} dv_L^{t+1}(i,j) &= wv_L^t(i,j) + c_1 r_1 \left(p_{bestL}^t(i,j) - x_L^t(i,j) \right) \\ &+ c_2 r_2 \left(Y_{bestL}^t(i,j) - x_L^t(i,j) \right) Y_{bestL} \\ &+ c_3 r_3 \left(g_{best}^t(i,j) - x_L^t(i,j) \right) \\ &i = 1,2,\cdots,N-E; \end{aligned} \tag{32}$$

where: $x_L^t(i,j)$ represents the j th dimension of the current position of particle i for the current inferior group. $p_{bestL}^t(i,j)$ is the j th dimension of particle i's p_{best}. The $Y_{bestL}^t(i,j)$ represents the j th dimension of the optimal particle. When the particle is the only one, the position of this particle is Y_{bestH}.

According to MOPSO for the population update without dynamic clustering, in order to keep the particles from leaving the search space, a restriction strategy is adopted on the boundary so that the updated particles still exist in the search space, and the following restriction strategy is adopted:

$$x^t(i,j) = \begin{cases} x_{\min}, & if\ x^t(i,j) < x_{\min} \\ x_{\max}, & if\ x^t(i,j) > x_{\max} \\ x^t(i,j), & elsewhere \end{cases} \tag{33}$$

where: $x_{\max}$, $x_{\min}$ are the maximum and minimum values of the search space, respectively.

(4) Optimal particle selection

An external archive is added to DCMOPSO and the non-dominated solutions generated by each population after independent optimization are recorded in the external archive. The part of the non-dominated solution with the smallest sparse distance is deleted when the capacity of the external archive reaches its limit.

During the evolution process, the age age of all non-dominated particles in the external archive is recorded, i.e., the number of consecutive generations of non-dominated particles in the external archive. In selecting the global optimum, the optional probabilities of all non-dominated particles are calculated, and then the non-dominated particle with the smallest probability and the largest sparse distance is selected as g_{best}. The probability is calculated as

follows:

$$p_i = age_i / Mage \tag{34}$$

where: for a non-dominated particle i, p_i is its optional probability. age_i is its age. $Mage$ then represents the maximum value of its age in the external file. For the high quality swarm as well as the low quality swarm, its optimal position is not static. Compare the position of each particle in the subgroup and find the particle with the best position, when there is only one in its number, the position of this particle is $Y_{bestH}\left(Y_{bestL}\right)$, on the contrary, if there are still other particles, then the largest particle is $Y_{bestH}\left(Y_{bestL}\right)$.

2.3.3 DCMOPSO Algorithm Involved in the Regulation Process

Step 1: Initialize U populations of size N and set the size N_{np} external archive.

Step 2: Evaluate each particle in terms of fitness and add non-dominated solutions to the external file.

Step 3: Randomly select the populations that need to control the execution dynamics and find the initial individual optimum of the particle, the global optimum p_{best}, and g_{best}.

Step 4: Apply the dynamic clustering strategy to the population. Merge the latest sub-populations to keep all particles in the search space according to Eq. (34).

Step 5: The particle p_{best} is conditioned while the external file is updated, and if no new particles are added to it, it will be differentially mutated. The new g_{best} is selected.

Step 6: The population for dynamic clustering in the next iteration is determined.

Step 7: When the condition is reached, the iteration stops. If not then return to step 4 to go to the next iteration, the flowchart of the algorithm of DCMOPSO is shown in Fig. 2.

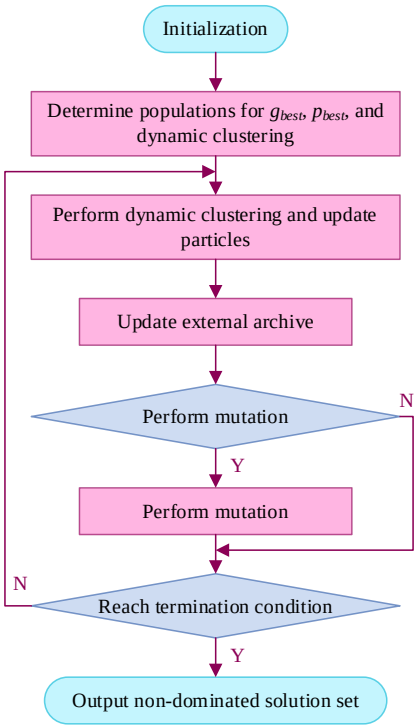

Figure 2: The algorithm flowchart of DCMOPSO

3 Results and Discussion

3.1 Basic data

In this paper, the experiments refer to the historical output of wind power and photovoltaic of a certain wind power station, and the IEEE-14 node system is used as an example to verify the validity of the model in this paper. The system is set up with 6 nodes of power generation stations and 8 nodes of large user loads, in which G1 on the power generation side is indicated as a wind power storage station, and the total capacity of wind power and PV within it is 300 MW, and G2-G6 are indicated as conventional thermal generating units, with the capacity of each unit being 350 MW, totaling 1,750 MW. The parameters of the energy storage are shown in Table 1. At the time of quotation, all the units on the generation side adopt 5-segment quotation, in which the capacity of each segment of conventional units is 70MW, and the quotation range of the wind and solar energy storage site at the time of decision-making is 140-600 yuan/(MW·h). Demand-side user's offer is also 5-segment, each segment capacity is 55MW, and the charging offer range of the wind energy storage station at the time of decision-making is also 140-600 yuan/(MW·h), and the offer parameters of the conventional unit and the system user are shown in Table 2. Both wind and solar storage field station regulation and market simulation are dispatched in 1-hour units.

Table 1: Energy storage parameters

Parameter name	Capacity	Charging and discharging efficiency	Self-depletion rate	Initial SOC	Charge and discharge depth
Numerical value	55MW/250(MW·h)	0.92	0.03	0.6	10%~85%

Table 2: Quotation parameters for conventional units and system users

	Number	Quotation in Paragraph 1(yuan/(MW·h))	Quotation in Paragraph 2(yuan/(MW·h))	Quotation in Paragraph 3(yuan/(MW·h))	Quotation in Paragraph 4(yuan/(MW·h))	Quotation in Paragraph 5(yuan/(MW·h))
Unit	G1	148.7	244.96	341.41	431.22	547.98
	G2	148.37	248.37	334.45	443.92	533.61
	G3	156.99	255.34	358.84	459.71	538.83
	G4	160.13	269.96	360.75	467.01	550.05
	G5	160.6	255.99	366.11	467.02	556.4
User	D1	450.36	415.53	331.25	216.59	78.4
	D2	471.79	388.52	329.79	177.6	132.34
	D3	542.35	444.54	296.56	191.05	115.61
	D4	468.45	350.53	340.02	228.73	53.43
	D5	480.81	384.86	332.3	237.54	86.73
	D6	507.41	354.15	315.74	172.14	83.47
	D7	532	424.47	339.82	243	95.4

3.2 Performance test of improved multi-objective particle swarm algorithm

In order to be able to verify the excellent performance of the improved particle swarm optimization algorithm proposed in this paper in comparison with different intelligent algorithms to deal with constrained optimization problems, this paper adopts 12 standard test functions as the test objects, which are run independently with the commonly used intelligent algorithms, such as the particle swarm optimization algorithm PSO, the differential evolutionary algorithm DE, the artificial bee colony algorithm ABC, the particle swarm optimization algorithm BPSO based on local search, the M classification artificial bee colony

Algorithm M-ABC and Adaptive Differential Evolution Algorithm ATMES are run independently. In order to ensure the validity of the comparison, the maximum number of function evaluations FFE_{max} of all algorithms is uniformly set to 30000.The detailed settings for the improved particle swarm optimization algorithms are as follows: the number of populations N=100, the inertia weights decrease linearly with the number of iterations from 0.8 to 0.5, the learning factor and are all set to 1.8, the scaling factor F is 0.7, and the crossover probability is 0.7.The various algorithms are each run independently for 50 times and the learning factor is set to 1.8. Each of the various algorithms are run independently for 50 times, and the results are statistically analyzed, and a comparison of the results of this paper's algorithms with other intelligent algorithms in the CEC2006 test function is shown in Table 3. The mean and variance of each algorithm are given in Table 3. "-" in the table means that the result is not obtained, and "NF" means that no feasible solution is found in the simulation. For the analysis of the comparison results in the table, the improved particle swarm optimization algorithm proposed in this paper obtains the optimal mean results on the eight test functions (g01, g04, g06, g08, g09, g10, g11, g12), and the overall mean level is better than that of the other comparison algorithms. Meanwhile, the IPSO algorithm not only obtains the optimal mean value on the six test functions of g06, g08, g09, g10, g11 and g12, but also the variance of the running results is the smallest, which shows the excellent performance of the algorithm, and further analyzing the test results of the improved particle swarm algorithm on the other standard test functions, due to the limitation of the number of populations of the improved algorithm and the linear change of inertial weights, it is not possible to jump out of the localized test function in the part of the test function, and the improved particle swarm algorithm can't jump out of the localized test function. There are some limitations due to the limitation of population size and linearly varying inertia weights of the improved algorithm that it is unable to jump out of the local optimal solution in some test functions. The excellent performance on most of the test functions shows the advantages of DCMOPSO in terms of accuracy and stability in dealing with constrained optimization problems.

Table 3: The algorithm compares with the results of his intelligent algorithm

Function	Indicators	Our	BLPSO	M-ABC	ATMES	PSO	DE	ABC
g01	Mean	−13	−8.67837	−13	−13	−17.61	−17.333	−13
	Variance	3.63E-16	0.63	0	0	–	–	-
g02	Mean	0.67078	−0.08060	−0.68833	−0.6866	−0.71886	−0.663	−0.6807
	Variance	--	--	0.00687	0.018	–	–	-
g03	Mean	0.88617	−0.16760	−1	−0.8888	0.66781	−1	−1
	Variance	--	0.173	0.00768	1E-7	–	–	–
g04	Mean	-30663.3	−30637.8	−30663.3	−30663.3	−30663.3	−30663.3	−30663.3
	Variance	8.88E-6	6.68	0	6.73E-10	–	–	–
g05	Mean	3181.383	3678.776	3168.138	3106.63	3133.863	3067.06	3183.617
	Variance	67.6	7.06	36.1	0.13	–	–	–
g06	Mean	-6861.81	−6761.68	−6861.81	−6861.81	−6861.81	−6837.73	−6861.81
	Variance	0	0.8	0	3.61E-10	–	–	–
g07	Mean	27.33786	133.6873	7.713	7.31736	30.706	7.31	7.763
	Variance	--	36	0.107	--	–	–	–
g08	Mean	-0.0838	−0.0838	−0.08380	−0.08380	−0.08380	−0.08380	−0.08380
	Variance	3.66E-18	8.7E-4	7.03E-16	6.1E-16	–	–	–
g09	Mean	695.63	613.0161	680.63	680.67	680.63	680.63	680.67
	Variance	8.06E-13	13.3	--	--	–	–	–
g10	Mean	6033.31	NF	6033.88	6066.76	6003.3	6176.337	6007.706
	Variance	11.8	NF	1.1	1.86	–	–	–
g11	Mean	0.6789	0.63	0.65	0.63	0.678	0.801	0.63
	Variance	1.13E-16	0.00183	3E-4	8E-8	–	–	–
g12	Mean	−1	−1	−1	−1	−0.88886	−1	−1
	Variance	0	5.33E-6	0	0	–	–	–

Further, according to the distribution of the mean values of the various algorithms in the table, the performance of different algorithms is ranked by average rank using Friedman's test statistic, and the comparison of the average rank ranking of different algorithms on the CEC2006 test function is shown in Fig. 3. As can be seen from the figure, the algorithm of this paper achieves the best ranked result among all the algorithms, and compared with PSO and DE algorithms, the performance of this paper's algorithm has been greatly improved, which illustrates the effectiveness of the improvement strategy proposed in this paper.

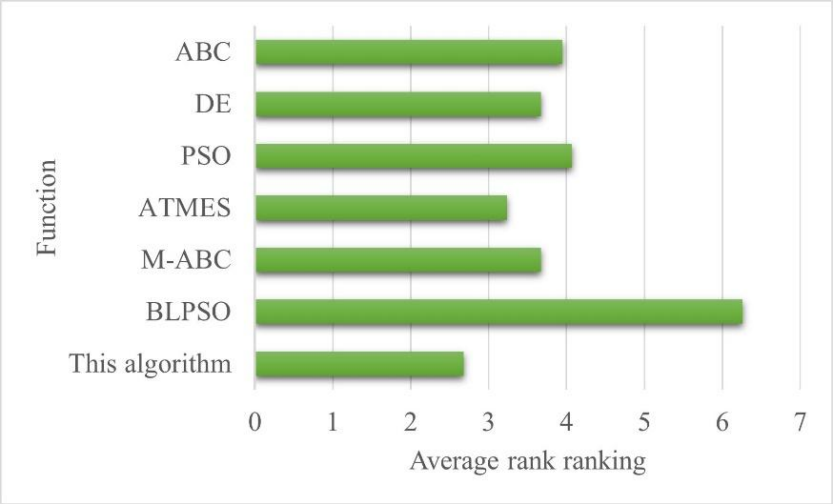

Figure 3: Average rank ranking comparison

At the same time, in order to compare and analyze the significance of the differences between various types of algorithms, this paper also adopts the Wilcoxon signed rank-sum test and analyzes the multi-problem test at a significant level of 5%.The comparison of the significance of the differences between DCMOPSO and other intelligent algorithms in the CEC2006 test function is shown in Table 4. “+” indicates that the IPSO algorithm is significantly better than the comparison algorithm, and “≈” indicates that there is no significant difference between the two algorithms. From the comparison results in the table, the analysis shows that IPSO performance is significantly better than BLPSO, PSO, DE and ABC algorithms, while there is no significant difference between DCMOPSO algorithm compared to ATMES and M-ABC.

Table 4: Significant difference comparison

Algorithm	R+	R-	Decision
BLPSO	228	0	+
M-ABC	179.5	82.5	≈
ATMES	122.5	132.5	≈
PSO	187	68	+
DE	189	45	+
ABC	210.5	42.5	+

In order to verify the robustness of the algorithm proposed in this paper, three representative g09 (polynomial term type), g11 (quadratic term type) and g12 (nonlinear type) in the test functions are selected for the box-plot comparisons.The distributions of the computational results of the IPSO algorithm and the other intelligent algorithms in the test functions of g09, g11 and g12 are shown in Figs. 4~6, respectively.Through the distributions of the box plots, it

can be seen that the improved particle swarm optimization algorithm produces objective function values that can be stably concentrated near the optimal solution compared with other intelligent algorithms. It can be seen that the improved particle swarm optimization algorithm produces objective function values that can be stably concentrated near the optimal solution compared to other intelligent algorithms, and IPSO has a smaller error distribution compared to other intelligent algorithms. Combining the above comparison results, the improved particle swarm optimization algorithm proposed in this paper has higher optimization accuracy and convergence stability compared with other intelligent algorithms such as BLPSO, M-ABC, ATMES, PSO, ABC, etc., which proves the excellence of the improved particle swarm optimization algorithm proposed in this paper for the solution of single-objective constrained optimization problems.

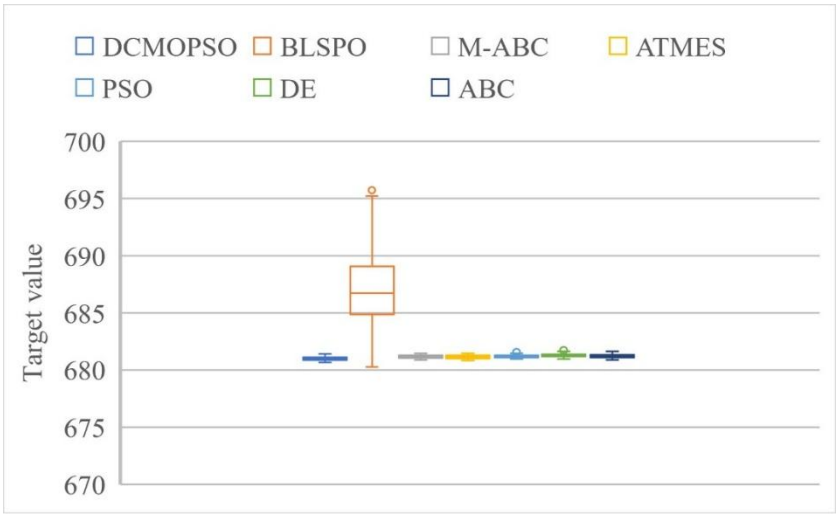

Figure 4: Box plots of the target values of the g09 test function for different algorithms

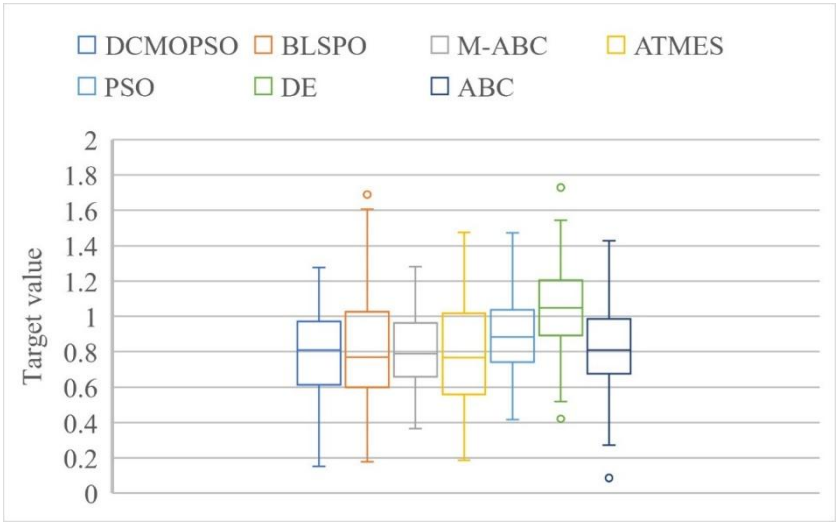

Figure 5: Box plots of the target values of the g11 test function for different algorithms

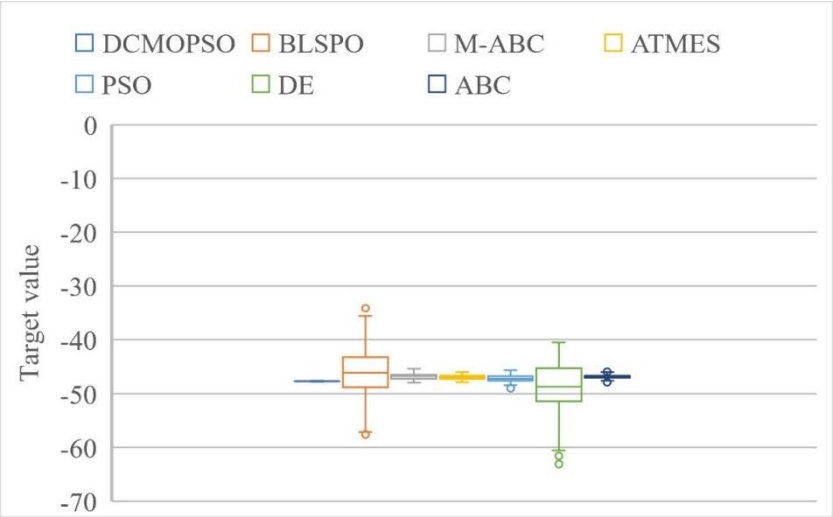

Figure 6: Box plots of the target values of the g12 test function for different algorithms

3.3 Application of regulatory strategies

3.3.1 Analysis of market decisions

In order to analyze the effectiveness of the proposed model in this section more clearly, the experiments are set up with REF scenario and DAM scenario respectively.The REF scenario indicates that the wind farms do not make the market offer decision, and participate in the day-ahead market with lower market offer: the DAM scenario is that the wind farms make the day-ahead market offer decision, and participate in the day-ahead market with strategic market strategy. In order to avoid the influence of unit location on the scheduling results, the influence of network blocking is ignored in the calculation, and SMP is used to analyze the algorithms.The cumulative power supply curves of the REF scenario and the DAM scenario are shown in Fig. 7.Figures (a) and (b) show the power generation offer of the wind farms of the REF scenario and DAM scenario, respectively, and Figs. (c) and (d) show the charging offer of the wind farms of the REF scenario and the DAM scenario, respectively. In Fig. (a), the wind farm participates in the market with a lower offer, while in the DAM scenario, the wind farm will participate in the day-ahead market with a higher market offer after its own market decision, and the market price of electricity will increase as its own offer increases.

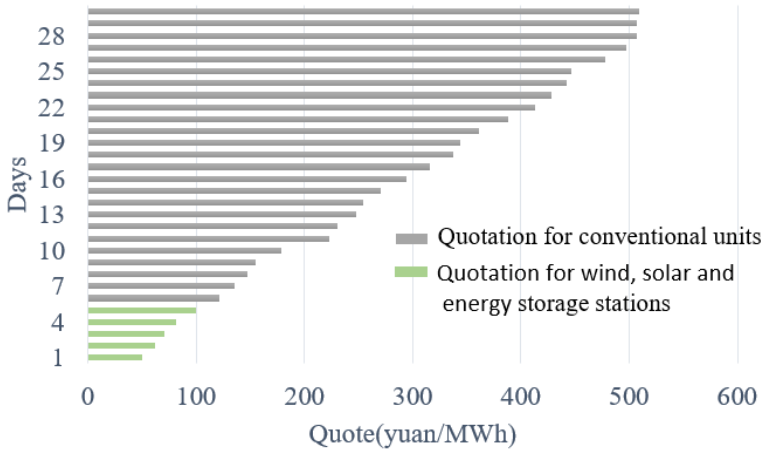

(a) Quotation for power generation of wind-solar-storage stations in REF scenarios

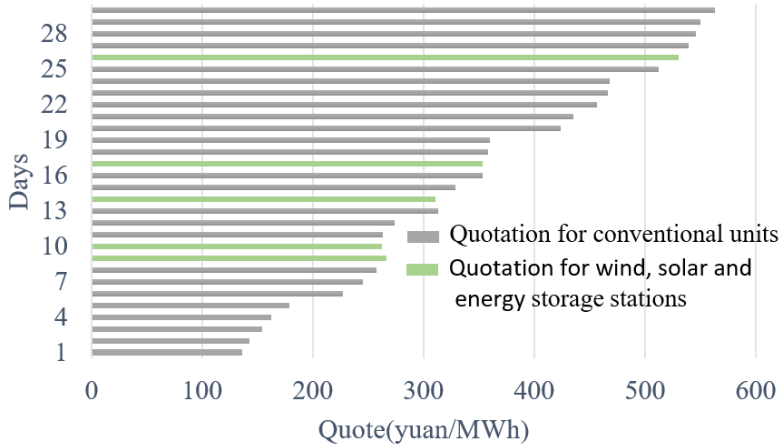

(b) Quotation for power generation of wind, solar and storage stations

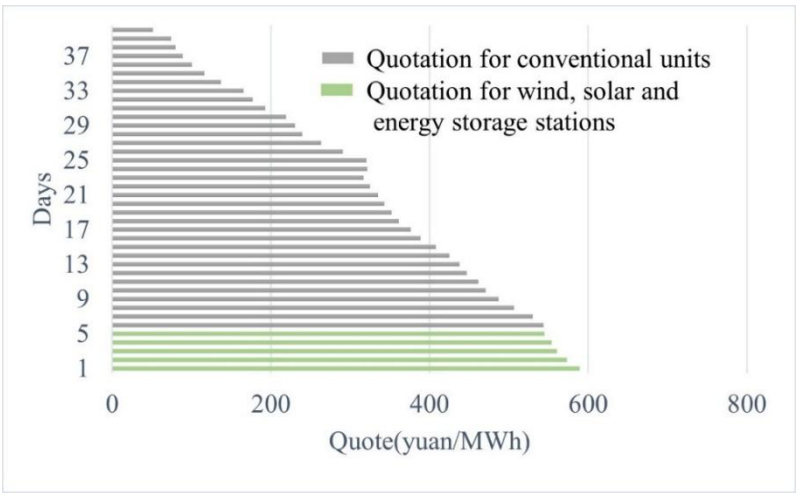

(c) REF scenario wind-solar-storage station charging quotation

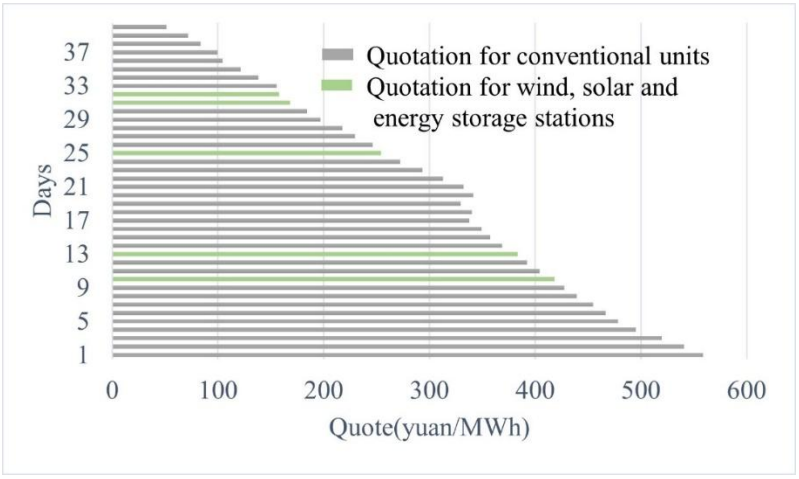

(d) Charging quotation for DAM scene wind-solar-storage station

Figure 7: The cumulative supply and electric curve of REF and DAM

REF, DAM scenario of wind energy storage site decision-making offer is shown in Figure

8. With the market decision of the wind energy storage site, its market offer is significantly increased, at t=3, the market offer is lifted from the low offer to 335.05 Yuan/MW, and the system SMP is also lifted from 250.22 Yuan/MW to 335.05 Yuan/MW, at this time, the G3 and the wind energy storage site are used as the marginal unit. At t=14, the market offer rises from the low offer to 550.56 Yuan/MW, and the system SMP also rises from 530.45 Yuan/MW to 550.56 Yuan/MW, and at this time, G4 and the wind storage field station act as the marginal unit. The market decision of the charging station is consistent with the generation, in the REF scenario, the wind power storage station will participate in the market as a user with a higher charging offer in order to clear all the electricity, while after the market decision of DAM, the wind power storage station will appropriately reduce its own charging offer in order to influence the marginal clearing electricity price in the market. Therefore, it can be seen that the DAM's market offer decision will improve its own market competitiveness by changing its own market offer, which will raise the market price of electricity and improve its own revenue, and the DAM will follow the other marginal unit's offer at the time of its decision.

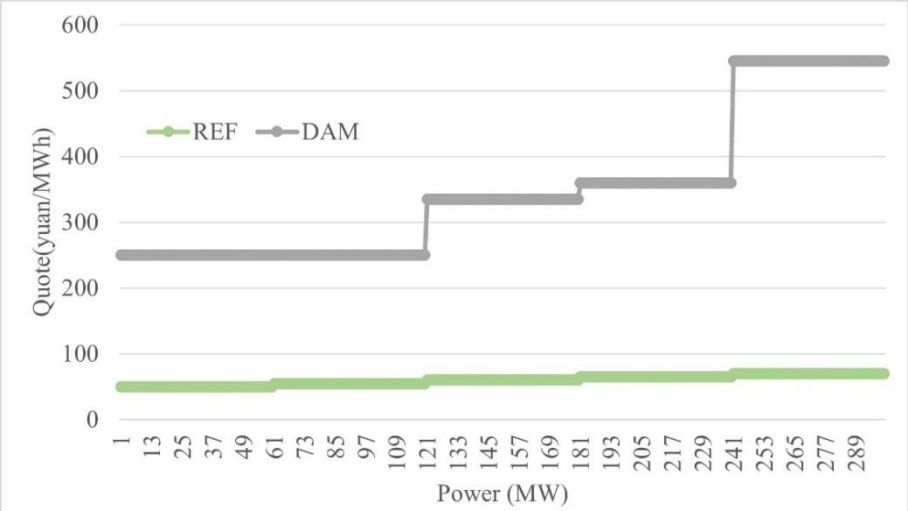

Figure 8: Decision-making quotations for wind-solar-storage stations in REF and DAM

The REF Scenario and DAM Scenario system SMPs and system loads are shown in Figure 9. The market is cleared according to the system load in each time period, and when the system load is lower, the capacity of the units available for bidding is smaller, and the SMP of the system after clearing will be lower. When the system load is high, the capacity of the units in the system that can be awarded bids is larger, and the SMP of the system after clearing will be higher, so the trend of system load and SMP is basically the same. In the REF scenario the wind energy storage site does not make market decisions, and the market SMP is determined by the conventional thermal power units, but with the market decisions of the wind energy storage site in the DAM, the system SMP will also be affected by the offer price of the wind energy storage site, and in order to improve its market revenue, the site will raise its own market offer price to raise the system SMP, so that the SMP of the DAM scenario is higher than that of the REF scenario as a whole in the figure. Scenario. Therefore, the SMP of the DAM scenario is higher than that of the REF scenario. The market revenue of the DAM scenario is also increased from 1.7253 million yuan in the REF scenario to 1.7859 million yuan in the DAM scenario.

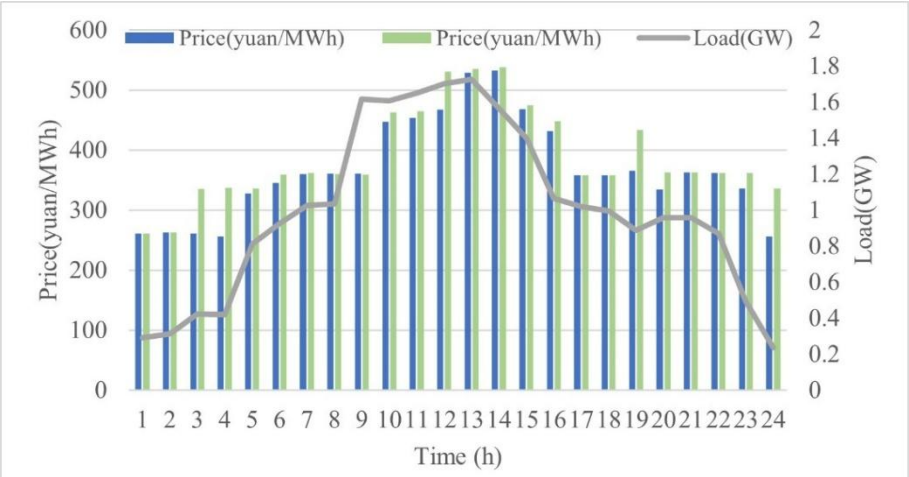

Figure 9: The system SMP and system load of the REF scenario and DAM scenario

3.3.2 Analysis of internal regulation

The output of the wind and energy storage station is mainly regulated by the energy storage inside the wind and energy storage station. The output power of wind and energy storage as well as the SOC of energy storage inside the wind energy storage field station under the market decision is shown in Fig. 10. Due to the market decision of the wind energy storage field station, the winning power of the field station needs to be calculated through the market clearing, so the field station needs to be charged and discharged by the energy storage to meet the winning power issued by the market. For example, in t=1~2 time period, the winning power of wind power storage station needs to meet the 128MW, the wind power of the station is larger in this time period, and the remaining power can be charged into the energy storage on the basis of meeting the winning bid, which reflects the wind power regulation ability of energy storage. In the t = 10 ~ 16 time period, the wind storage station needs to meet the winning power of 242MW, the wind power of the station is not enough to meet its own winning bid, so the time period needs to be discharged into the energy storage to supplement its own power, but the energy storage can not meet the demand of the station only by relying on the charging of the wind, so the energy storage needs to be purchased externally in the time period of t = 1 ~ 2 and t = 9, which embodies the arbitrage behavior of the energy storage. In addition, the SOC of energy storage changes continuously with the charging and discharging of energy storage, and in the time period of t = 10 to 16, energy storage discharges externally to satisfy the winning bid of the field station, and the SOC of energy storage in this time period gradually decreases with the discharging of energy storage.

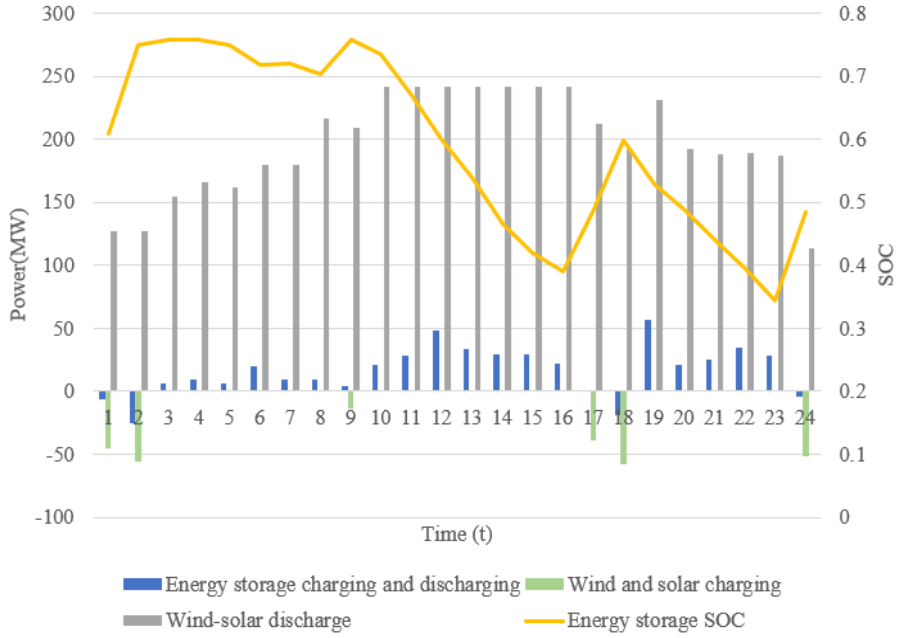

Figure 10: DAM scenario lower wind light storage station and energy storage SOC

The total output of the wind energy storage stations in the REF scenario and the DAM scenario as well as the system SMP are shown in Fig. 11. Since the wind energy storage stations aim at maximizing their own revenue when making decisions, the stations tend to put out their power in the high tariff hours, and it can be seen from the figure that the change trend of the station's output is basically the same as the trend of the change of the tariff. Comparing the output of REF scenario and DAM scenario, it can be found that the output of wind storage stations in DAM scenario is generally higher than that of REF scenario in high tariff hours, such as t = 10-16 hours. In contrast, the DAM scenarios have smaller outputs in certain low tariff periods such as t = 1 to 2. In addition, the total output of wind power stations in the DAM scenario is 4697.55 MW, while the total output of stations in the REF scenario is 4578.69 MW. Therefore, wind power storage stations can effectively regulate their own outputs internally, and energy storage can effectively regulate the wind power outputs and carry out effective arbitrage behaviors according to the price of electricity.

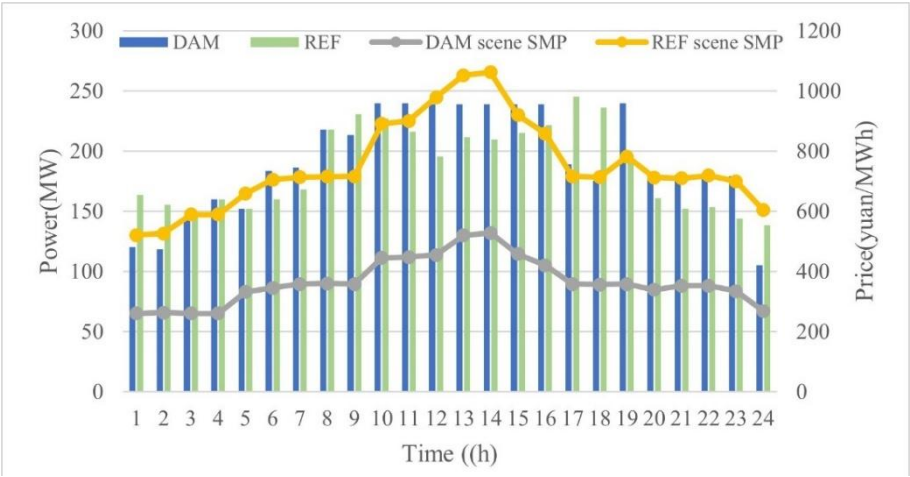

Figure 11: The total output of the wind-solar-storage station and the system SMP

4 Conclusion

In order to realize the cooperative regulation of aggregated power subjects and their market decision-making, this paper constructs an optimized regulation model of power market transaction and solves it by using the improved multi-objective particle swarm algorithm. The following conclusions are obtained through simulation and analysis:

(1) In the performance test experiment of the improved multi-objective particle swarm algorithm, the improved particle swarm optimization algorithm proposed in this paper obtains the optimal mean value results in the test functions of g01, g04, g06, g08, g09, g10, g11, g12, which is better than other comparative algorithms, which proves that the algorithm proposed in this paper has high optimization accuracy, fast convergence speed and other excellent performance.

(2) Experiments are conducted to verify the effectiveness of the regulation method proposed in this paper by taking the node system as an example. The example verifies the effectiveness of this paper's modeling method and the benefits under the market strategy decision: the strategic market decision of the field station can raise the market price of electricity and enhance its own market revenue. The internal regulation of the site can effectively adjust its own output to meet the winning bid and realize the arbitrage of energy storage.

References

[1] Heylen, E., Deconinck, G., & Van Hertem, D. (2018). Review and classification of reliability indicators for power systems with a high share of renewable energy sources. Renewable and Sustainable Energy Reviews, 97, 554-568.

[2] Kroposki, B., Johnson, B., Zhang, Y., Gevorgian, V., Denholm, P., Hodge, B. M., & Hannegan, B. (2017). Achieving a 100% renewable grid: Operating electric power systems with extremely high levels of variable renewable energy. IEEE Power and energy magazine, 15(2), 61-73.

[3] Liu, H., & Wang, Z. (2020). Research on energy storage and high proportion of renewable energy planning considering demand. IEEE Access, 8, 198591-198599.

[4] Yan, J., Liu, S., Yan, Y., Liu, Y., Han, S., & Zhang, H. (2024). How to choose mobile energy storage or fixed energy storage in high proportion renewable energy scenarios: Evidence in China. Applied Energy, 376, 124274.

[5] Zhang, N., Yu, Y., Wu, J., Du, E., Zhang, S., & Xiao, J. (2024). Optimal configuration of concentrating solar power generation in power system with high share of renewable energy resources. Renewable Energy, 220, 119535.

[6] Opeyemi, B. M. (2021). Path to sustainable energy consumption: The possibility of substituting renewable energy for non-renewable energy. Energy, 228, 120519.

[7] Song, J., Zhou, X., Zhou, Z., Wang, Y., Wang, Y., & Wang, X. (2023). Review of low inertia in power systems caused by high proportion of renewable energy grid integration. Energies, 16(16), 6042.

[8] Kasaei, M. J., Gandomkar, M., & Nikoukar, J. (2017). Optimal management of renewable

energy sources by virtual power plant. Renewable energy, 114, 1180-1188.

[9] Marinescu, B., Gomis-Bellmunt, O., Dörfler, F., Schulte, H., & Sigrist, L. (2022). Dynamic virtual power plant: A new concept for grid integration of renewable energy sources. IEEe Access, 10, 104980-104995.

[10] Lin, Y., Lin, W., Wu, W., & Zhu, Z. (2023). Optimal scheduling of power systems with high proportions of renewable energy accounting for operational flexibility. Energies, 16(14), 5537.

[11] Shi, Z., Wang, W., Huang, Y., Li, P., & Dong, L. (2020). Simultaneous optimization of renewable energy and energy storage capacity with the hierarchical control. CSEE Journal of Power and Energy Systems, 8(1), 95-104.

[12] Zhou, Y., Wang, C., Wu, J., Wang, J., Cheng, M., & Li, G. (2017). Optimal scheduling of aggregated thermostatically controlled loads with renewable generation in the intraday electricity market. Applied energy, 188, 456-465.

[13] Vulic, N., Rüdisüli, M., & Orehounig, K. (2023). Evaluating energy flexibility requirements for high shares of variable renewable energy: A heuristic approach. Energy, 270, 126885.

[14] Bessa, R., Moreira, C., Silva, B., & Matos, M. (2019). Handling renewable energy variability and uncertainty in power system operation. Advances in Energy Systems: The Large-scale Renewable Energy Integration Challenge, 1-26.

[15] Montoya-Bueno, S., Muñoz-Hernández, J. I., & Contreras, J. (2016). Uncertainty management of renewable distributed generation. Journal of Cleaner Production, 138, 103-118.

[16] Alonso-Travesset, À., Coppitters, D., Martín, H., & de la Hoz, J. (2023). Economic and regulatory uncertainty in renewable energy system design: A review. Energies, 16(2), 882.

[17] Feng, B., Fu, Y., Huang, Q., Ma, C., Sun, Q., & Wennersten, R. (2023). Multi-objective optimization of an integrated energy system with high proportion of renewable energy under multiple uncertainties. Energy Reports, 9, 695-701.

[18] Pata, S. K. (2024). Comparative impacts of energy, climate, and economic policy uncertainties on renewable energy. Journal of Environmental Management, 370, 122494.

[19] Abdullah, M. A., Muttaqi, K. M., & Agalgaonkar, A. P. (2015). Sustainable energy system design with distributed renewable resources considering economic, environmental and uncertainty aspects. Renewable Energy, 78, 165-172.

[20] Li, Y., Li, Y., Song, Z., & Ma, Z. (2025). The research on resilient power system construction for high-proportion renewable energy: Responsiveness enhancement and intelligent development pathways. Advances in Resources Research, 5(3), 1381-1421.

[21] Qi, S., Li, D., Hou, L., Wang, H., Xin, L., Jin, Y., ... & Ban, M. (2025). Two-Stage Robust Optimization Considering the Uncertainty of Sources and Loads in Virtual Power Plants. IEEE Access.